Collapse and accretion of ancient seamounts : a Jurassic example from the Mino terrane,the Suzuka Mountains,central Japan

山縣, 毅

https://doi.org/10.11501/3075545

出版情報：九州大学, 1993, 博士（理学）, 論文博士
バージョン：
権利関係：

Plate 1

Plate 1 Basaltic rocks of the Suzuka unit. Localities are shown in Fig. 6.

A. Outcrop view of pillow lava from block of basaltic rocks embedded in broken basalt-breccia.

B. Photomicrograph of porphyritic basalt with phenocrysts of plagioclase (pl) and clinopyroxene (cpx). Polars crossed. Scale bar: 1mm.

C. Photomicrograph of dolerite lava. Polars crossed. pl : plagioclase, cpx : clinopyroxene. Scale bar represents 1mm.

D. Photomicrograph of hyaloclastite characterized by vesicular shards with a small amount of subhedral plagioclase laths. Polars not crossed. Scale bar represents 1mm.

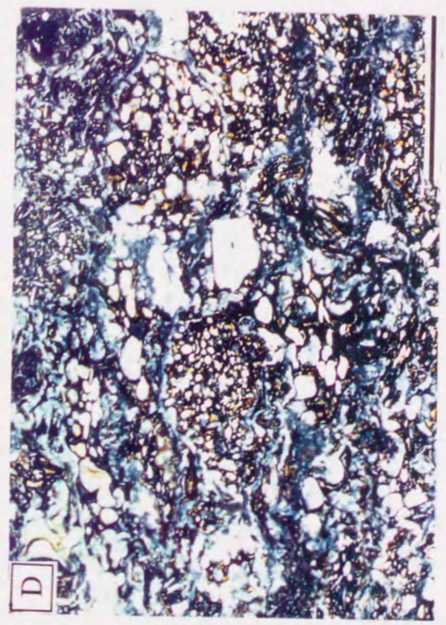

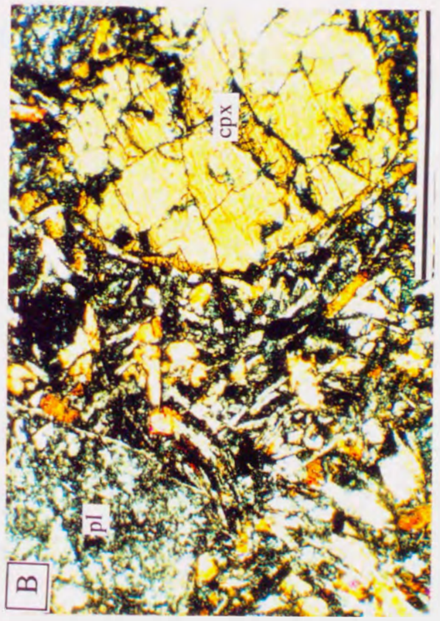

Plate 2

Plate 2 Shallow-marine limestone of the Suzuka unit. Localities are shown in Fig. 6.

A. Outcrop view of black bedded limestones of the lower member of the shallow-marine limestone succession.

B. Outcrop view of gray to light gray, massive limestone of the middle member of the shallow-marine limestone succession.

C. Photomicrograph of the limestone-breccia. Polymictic limestone-breccia has angular, unsorted limestone lithoclasts chaotically embedded in a well-sorted lime-mud matrix. Lithoclasts are supported by one another. mtx.: lime-mud matrix, m.: bioclastic lime-mudstone, g.: algal lime-grainstone. Plane light. Scale bar: 2.5 mm.

D. Photomicrograph of the limestone-breccia. Lithoclasts of lime-mudstone (a) and bioclastic lime-mudstone (b) are bounded by stylolite seams. Plane light. Scale bar: 2.5 mm.

Plate 3

Plate 3 Photomicrographs of the shallow-marine limestone. Plane light.

All scale bars: 2.5 mm. Localities are shown in Fig. 6.

A. Peloidal lime-mudstone. Minute bioclastic debris are scattered in a peloidal lime-mud matrix.

B. Bivalve lime-wackestone with a poor-sorted peloidal lime-silt matrix. Most of skeletal debris comprise bivalve shells. A small amount of ostracods and the small foraminifers is associated.

C and D. Bioclastic lime-wackestone. Red algae form thin veneers of algal mat.

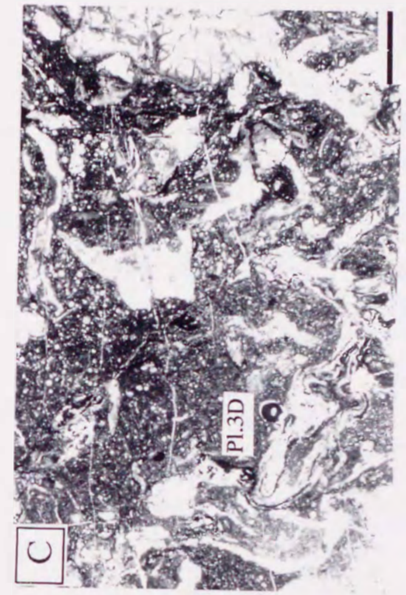

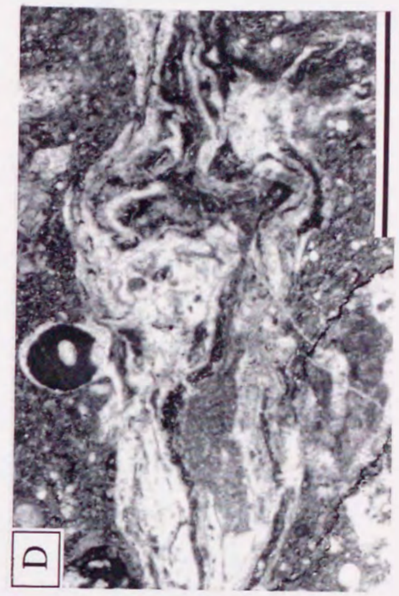

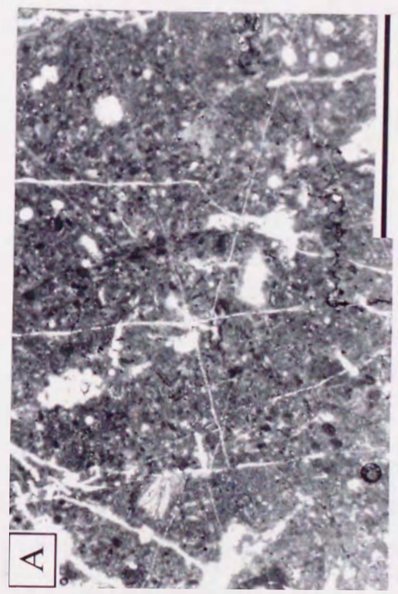

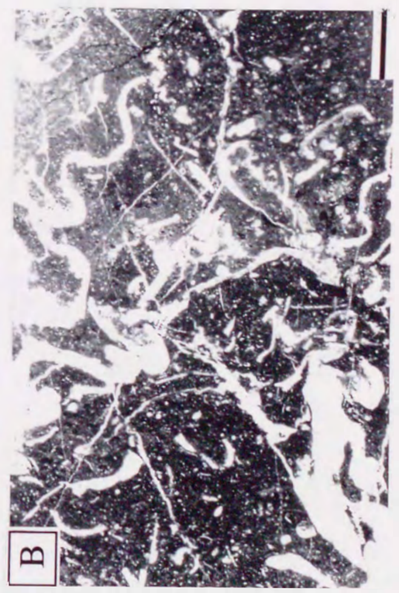

Plate 4

Plate 4 Photomicrographs of the shallow-marine limestone. Plane light.

All scale bars: 2.5 mm. Localities are shown in Fig. 6.

A. Bioclastic lime-mud/wackestone. Skeletal debris include the small foraminifers, thin-shelled bivalves, calcispheres, ostracods, and cyanobacterias, all embedded in a poor-sorted bioclastic lime-silt matrix.

B. Peloidal lime-grainstone. Well-sorted peloids are dense-packed and cemented by recrystallized sparry calcite. Rounded, cylindrical-shaped peloids are probably derived from girvanellid cyanophytes.

C. Oolitic lime-grainstone. Nuclei of ooids comprise sparry carbonate grains, peloids and crinoids.

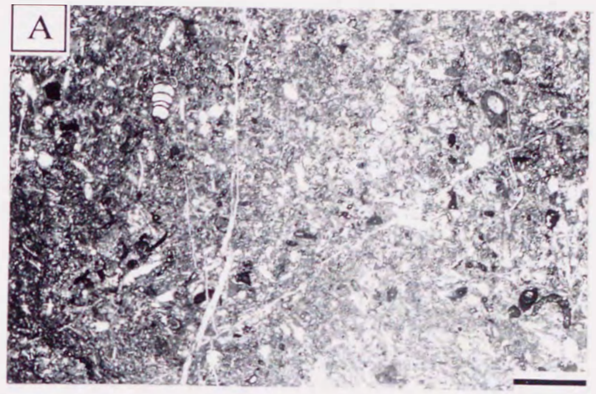

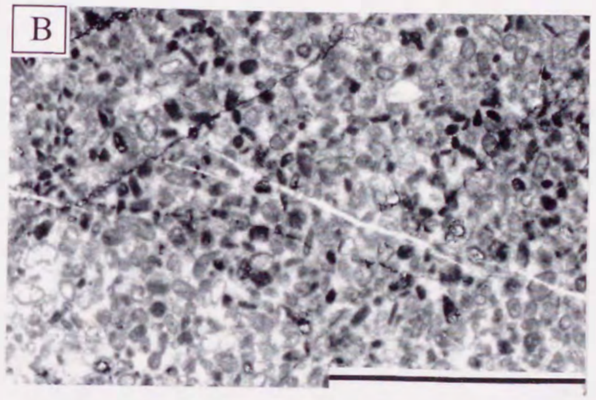

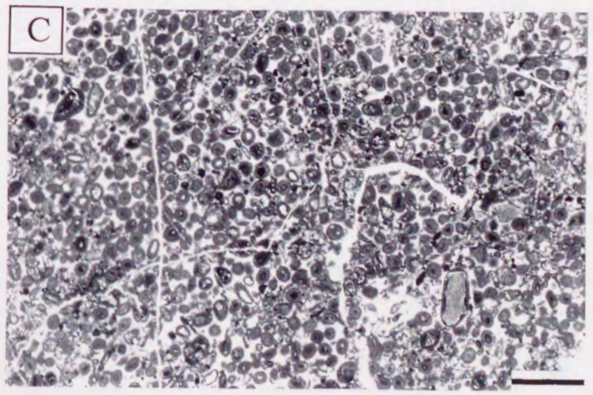

Plate 5

Plate 5 Photomicrographs of the shallow-marine limestone. Plane light.

All scale bars: 2.5 mm. Localities are shown in Fig. 6.

A. Crinoid-fusuline lime-wacke/packstone. Fusulines and a small amount of crinoids are largely supported by each other.

B. Crinoid-fusuline lime-wackestone. Note local pulverization into cloudy lime-paste, denoted by arrow.

C. Crinoid-fusuline lime-wackestone. A large amount of minutetubes is contained in lime-wackestone. They are probably calcareous algae.

Plate 5

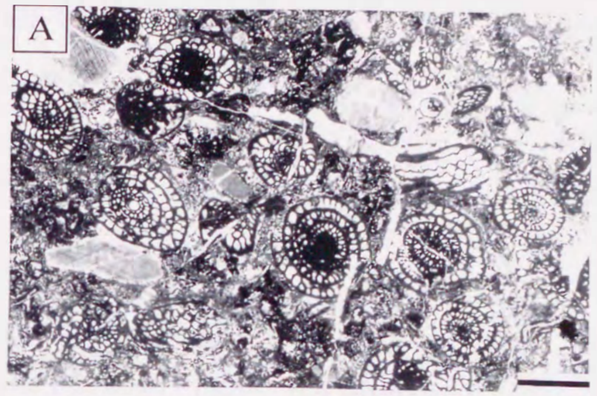

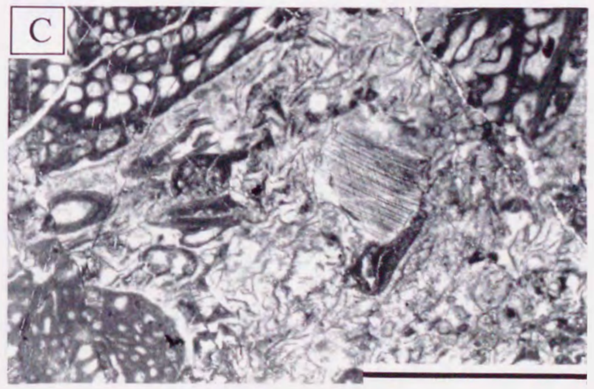

Plate 6

Plate 6 Photomicrographs of the shallow-marine limestones. Plane light.

All scale bars: 2.5 mm. Localities are shown in Fig. 6.

A. Algal lime-wackestone. Most of skeletal debris are cyanophytes. A small amount of calcispheres, the small foraminifers, bivalves, and peloids is discerned.

B. Algal lime-wackestone. Short tubes are cyanophytes. Close-up view of Plate6A.

C. Fusuline peloidal lime-grainstone. Fusulines, a large mass of cyanophytes, and diverse skeletal particles are dense-packed within peloidal matrix. Local sparry cements occur.

D. Fusuline peloidal lime-grainstone. Fusulines and crinoids are coated by algal micrite.

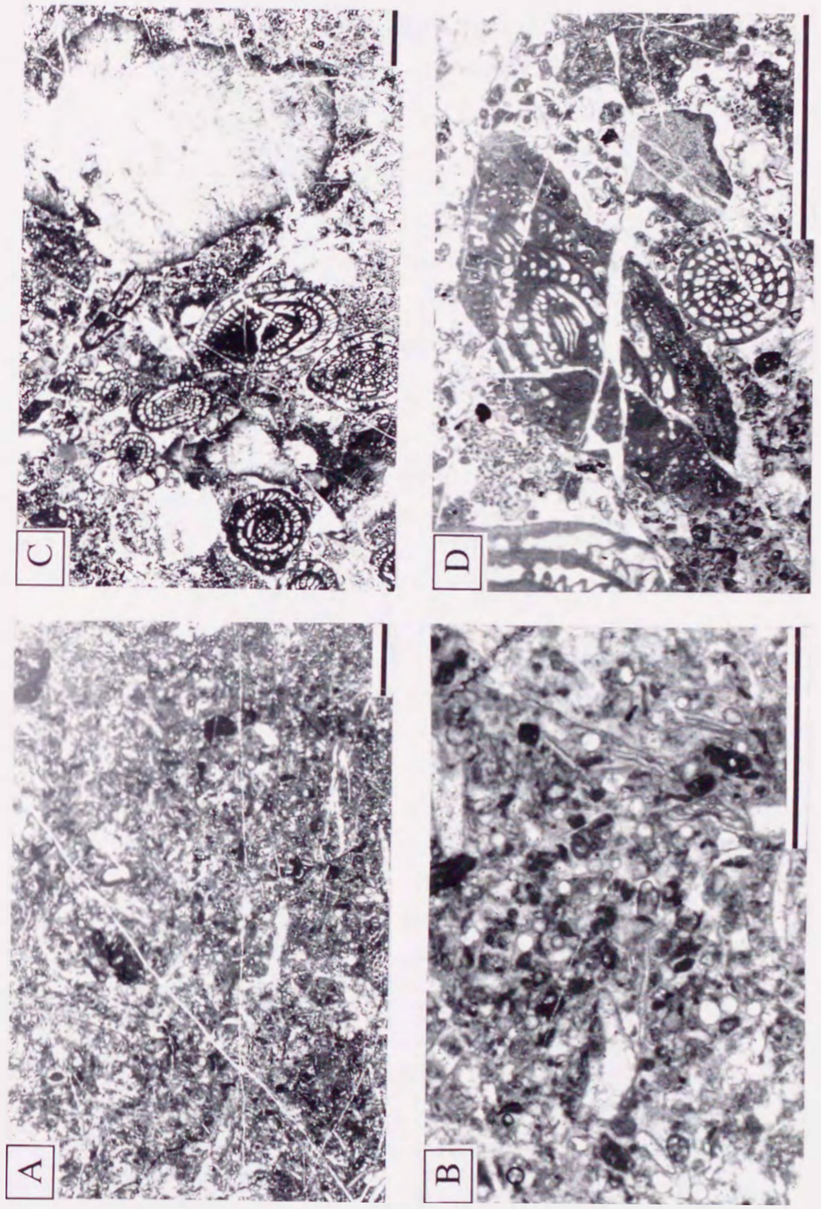

Plate 7

Plate 7 Photomicrographs of the shallow-marine limestone. Plane light.

All scale bars: 2.5 mm. Localities are shown in Fig. 6.

A. Algal bindstone with primary open-spaces filled by sparry calcite. Cyanobacterias bindstone is encrusted by red algae.

B. Cyanobacterias algal bindstone. Rock framework incorporates fusulines, green algae, bivalves, and the smaller foraminifers. Open spaces are filled by sparry calcite. Close-up view of Plate7A.

C. Red algae, probably *Archaeodispoleum* forms algal mats consisting of alternating micrite layers and layers of sparry calcite. Close-up view of fine lamellar structure in Plate7A.

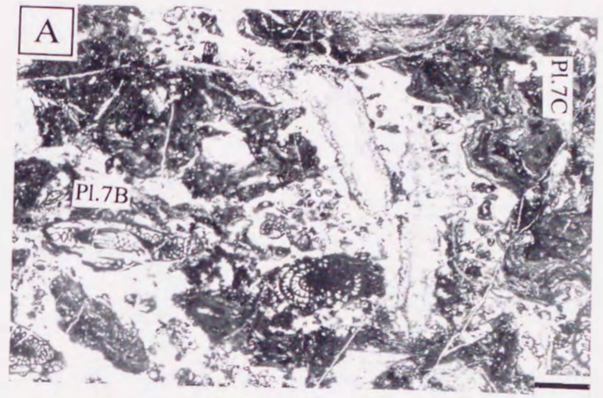

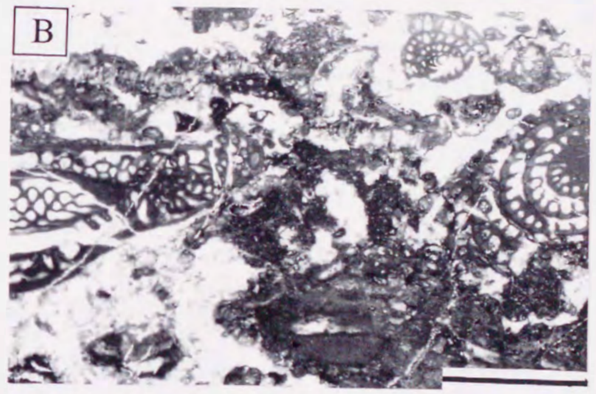

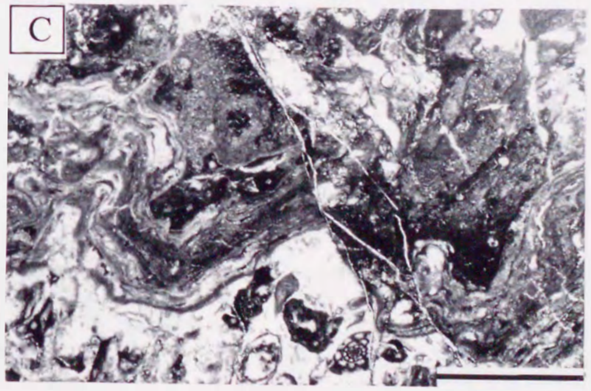

Plate 8

Plate 8 Polished slabs of Permian allochthonous limestones. All scale bars: 2 cm. Localities are shown in Fig. 6.

A. Bedded reworked lime-mudstone containing a large amount of heavily micritized fusuline debris. Wavy- laminated reworked lime-mudstone (b) is overlain by normally graded lime-mudstone (a).

B. Reworked lime-packstone containing a large amount of fusuline debris.

C. Volcaniclastic mudstone. Clasts of fusulines (black) and crinoids (white) are randomly scattered in a volcaniclastic matrix.

D. Bedded limestone-sandstone containing fusuline debris. The two beds of limestone-sandstone (a) and (b) show grading lamination.

C

D

A

B

Plate 9

Plate 9 Photomicrographs of Permian allochthonous limestones. Plane light.

All scale bars: 2.5 mm. Localities are shown in Fig. 6.

A. Reworked lime-mudstone, which consists of sand-sized grains of sparry calcite with a lime-mud matrix. Most of skeletal debris are foraminifers.

B. Reworked lime-packstone. Clasts of fusulines and crinoids are densely packed, supported by one other and embedded in a very fine lime-mud matrix.

C. Volcaniclastic mudstone containing calcite grains less than silt-size and clasts of fusuline and brachiopod disseminated within a volcaniclastic clay-rich, fine-grained matrix.

D. Limestone-sandstone characterized by well sorted sand-sized grains of sparry to microsparry calcite, which shows normal grading.

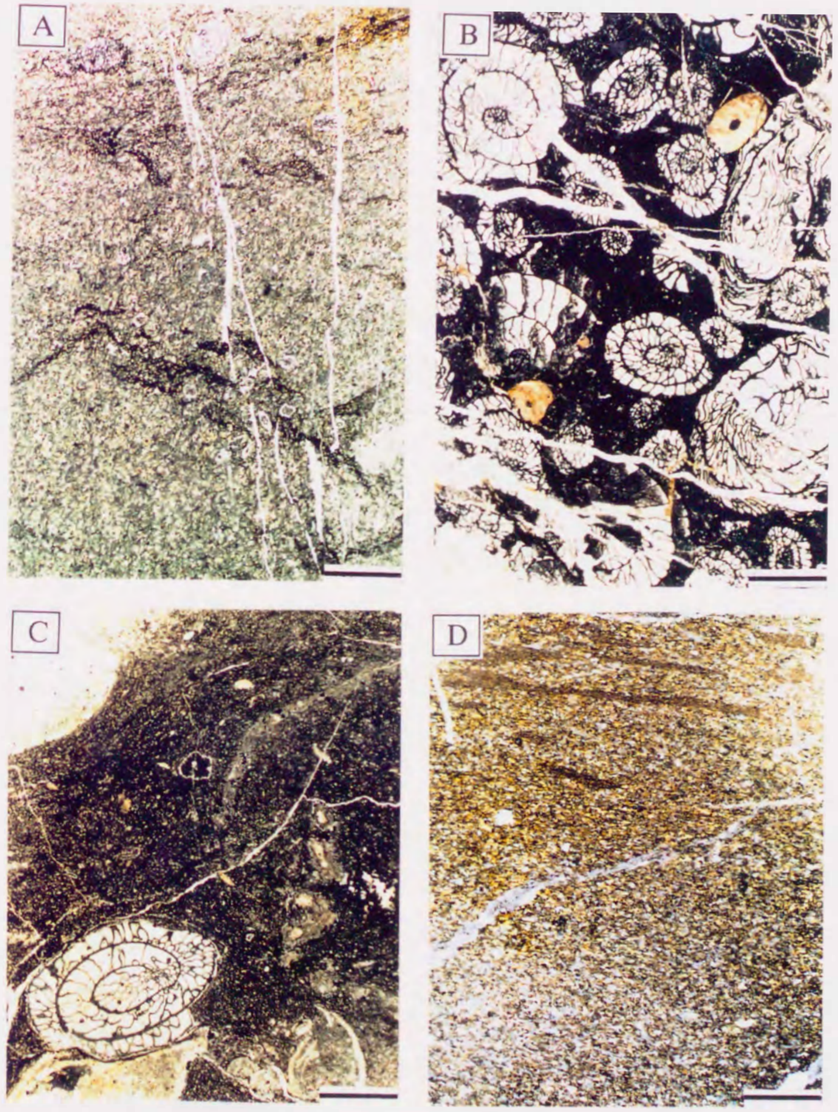

Plate 10

Plate 10 Photomicrographs of Permian allochthonous limestones. Plane light. All scale bars: 2.5 mm. Localities are shown in Fig. 6.

A. Limestone-basalt conglomerate. Clasts of limestone, vesicular glassy basalt, and isolated skeletal debris including fusulines and crinoids are densely packed by a volcaniclastic mud matrix. Limestone clasts have irregularly rugged outlines due to intense stylolitization.

B. Limestone-basalt conglomerate. Abraded clasts of basalt are dense-packed, supported by each other and cemented by sparry calcite together with a small amount of fragmented fusulines and crinoids.

C. Reworked lime-packstone flattened by overloading of rock fall deposits.

D. Fusulines destructed by loading of rock fall deposits in reworked lime-packstone. Walls and septa of fusulines were squashed in brittle manner. Close-up view of Plate 10C.

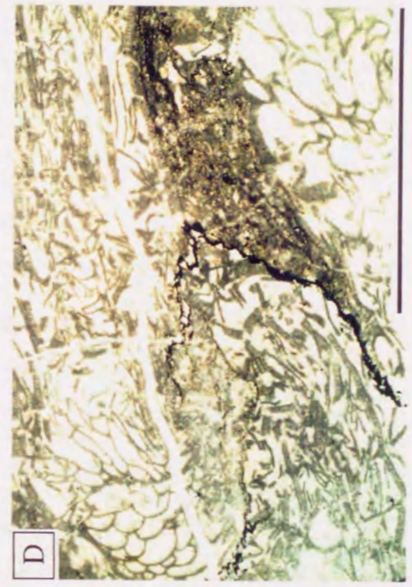

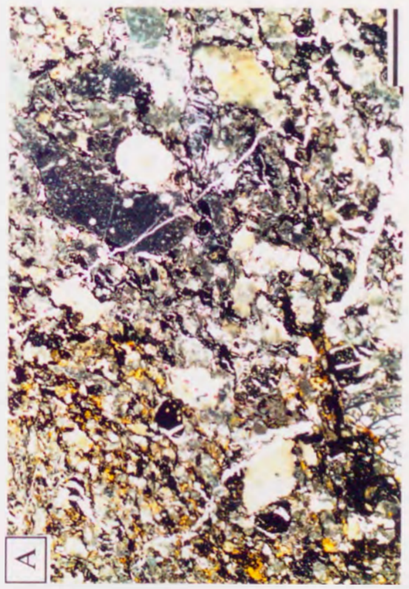

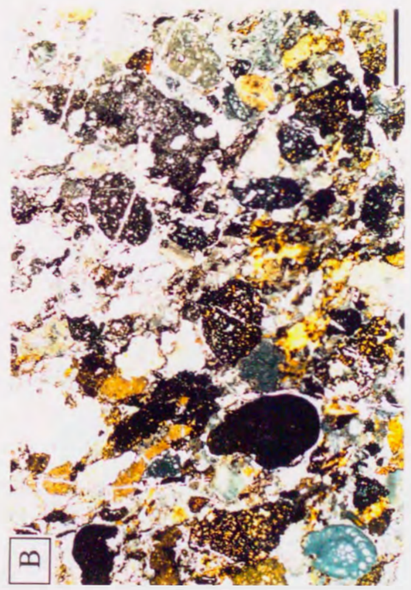

Plate 11

Plate 11 Limestone replaced into Jurassic chert of the Suzuka unit.

A. Polished slab of the deep-marine limestone-conglomerate. Poorly sorted, disorganized, angular clasts of micritic limestone (white) are set in a micritic matrix (gray), both rock-types containing radiolarian remains. Scale bar: 2 cm. Locality is shown in Fig. 12.

B. Photomicrograph of deep-marine limestone-conglomerate containing clasts of radiolarian biomicrite (ls.) and chert (ch.) set in micritic matrix (mtx.) with radiolarian remains and sand-sized debris of sparry calcite (cal.). Polars crossed. Scale bar: 1 m. Locality is shown in Fig. 12.

C. Permian limestone-breccia embedded in Jurassic chert. Locality is shown in Fig. 13.

D. Polish slab of Permian limestone-breccia embedded in Jurassic chert. Limestone-breccia comprises clasts of Permian limestones and lime-mud matrix. Scale bar: 2 cm. Locality is shown in Fig. 13.

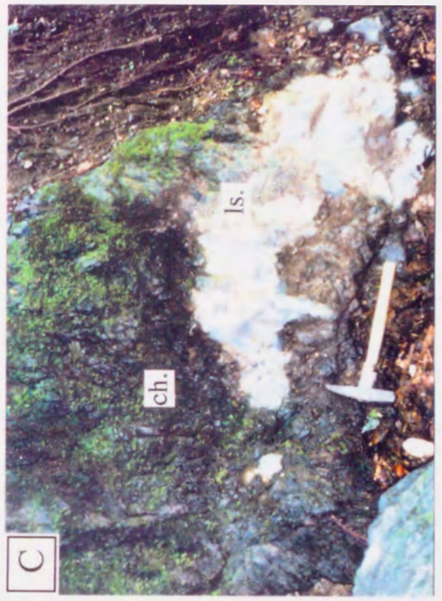

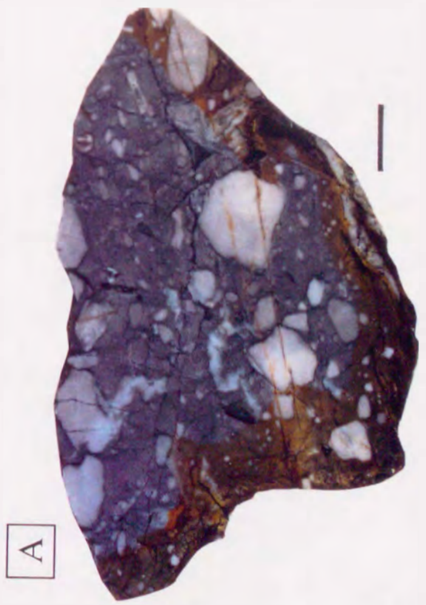

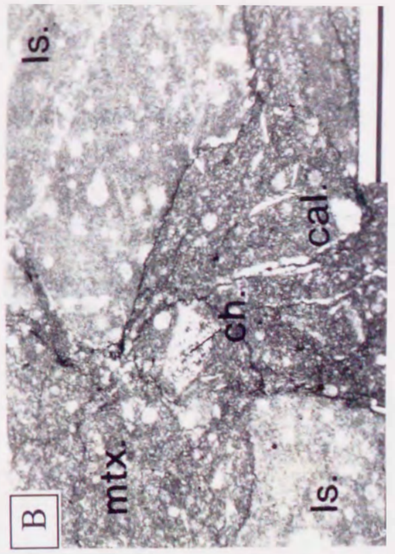

Plate 12

Plate 12 Polished slab and its line-drawing interpretation of destruction fabric in basalt lava. The light green destruction parts are randomly distributed. p: parent rock, d: destruction products. Scale bar 2 cm. Locality is shown in Fig. 6.

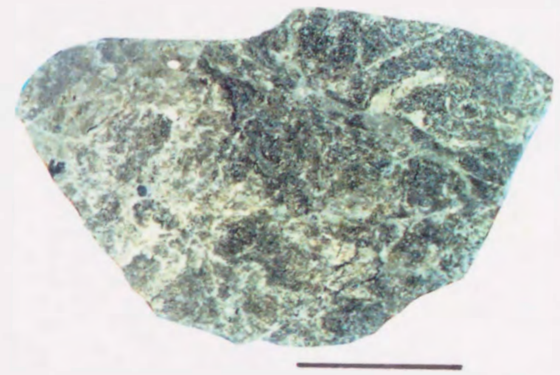

Plate 13

Plate 13

Plate 13 Photomicrographs and their line-drawing interpretation of destruction fabric in basalt lava. All scale bars: 1mm. Localities are shown in Fig. 6.

A. Cloudy and finely destruction products containing silt-sized fragments of plagioclase. Parent rock of basalt is brecciated into several rock-pieces. p: parent rock, d: destruction product. Plane light.

B. Pulverization products containing angular fragments of plagioclase. Note sharp contact with the parent rock. p: parent rock, d: destruction product. Polars crossed.

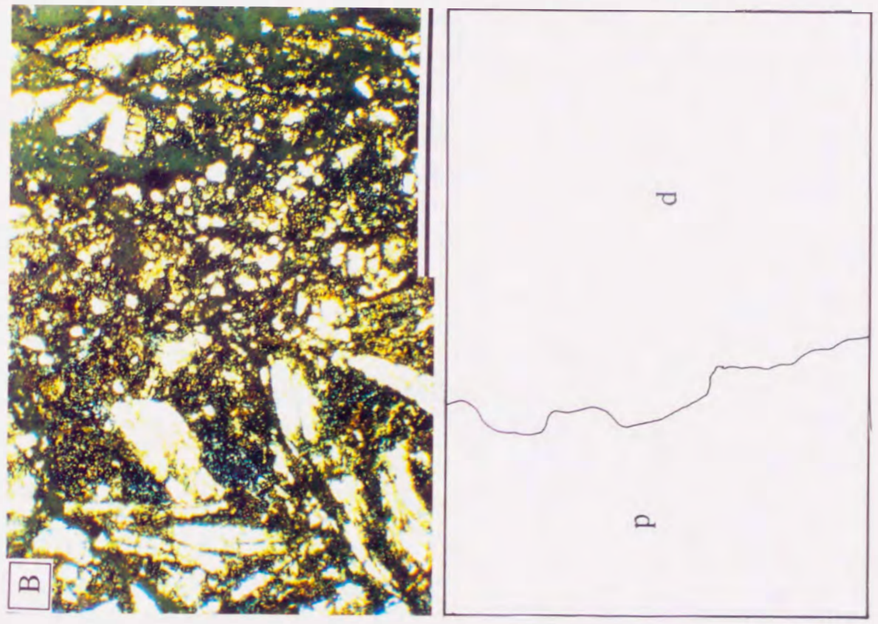

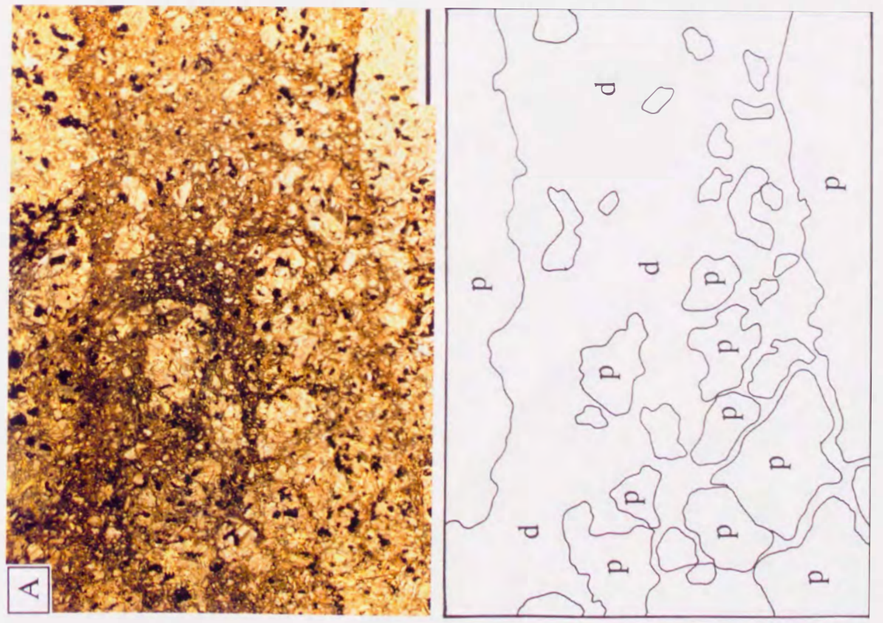

Plate 14

Plate 14 Photomicrographs of weak destruction fabrics of basaltic rocks.

All scale bars: 1mm. Localities are shown in Fig. 6.

A. Comminution and pulverization of plagioclase phenocrysts in porphyritic basalt lava. Plane light.

B. Close-up view of comminution of plagioclase phenocryst. Polars not crossed. The comminution fragments of plagioclase crowd around the parent phenocryst.

C and D. Pulverized and comminuted phenocryst of plagioclase. C: Polars not crossed, D: Polars crossed. Plagioclase phenocrysts are crushed into many smaller fragments, but not dispersed nor scattered.

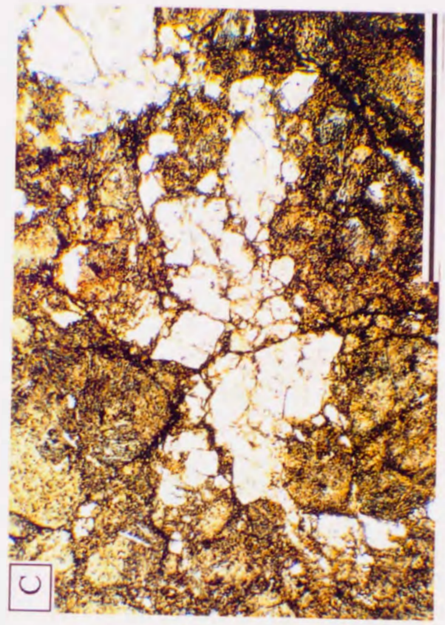

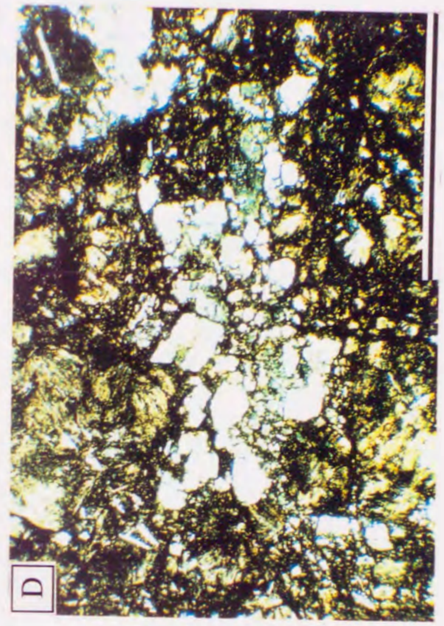

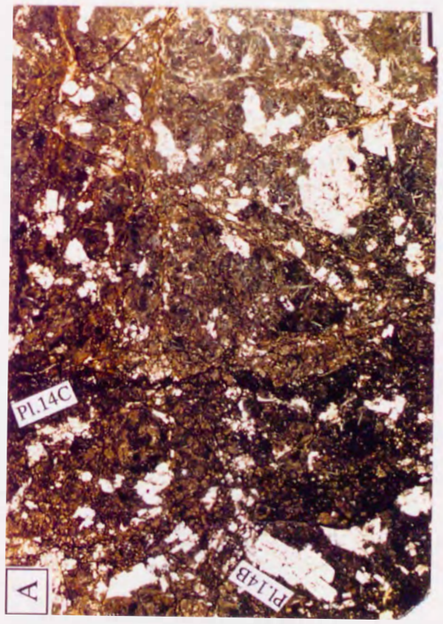

Plate 15

Plate 15 Photomicrographs of weak to moderate destruction fabrics in basaltic rocks. All scale bars: 1mm. Localities are shown in Fig. 6.

A. Weak destruction fabric in basalt lava. Dark parts lacking laths of plagioclase (indicated by black arrows) are the pulverization zones. Plane light.

B. Close-up view of pulverization zones containing fragments of plagioclase. Plane light.

C. Moderate destruction fabric in basalt lava. Parent rock of basalt is brecciated into several rock-pieces. Plane light.

D. Close-up view of cloudy and finely pulverized materials with numerous comminuted plagioclase fragments. Cross-polarized light.

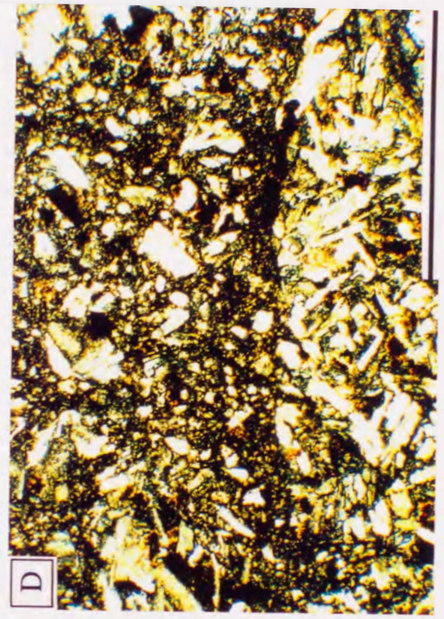

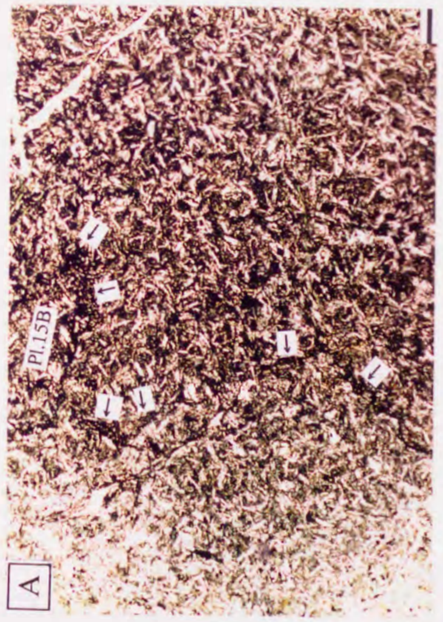

Plate 16

Plate 16 Photomicrographs of basalt lava having strong destruction fabrics.

All scale bars: 1mm. Localities are shown in Fig. 6.

A. Strongly crushed basalt lava. Rock-pieces of basalt are isolated in fine pulverization products with plagioclase fragments. Several rock-pieces can be reconstructed into a larger rock-piece. Plane light.

B. Angular to subrounded rock-pieces of basalt lava chaotically embedded in very fine pulverization products.

C. Close-up view of rock-pieces in pulverization products on Plate 16B. Outlines of basalt rock-pieces are usually sharp, but are locally difficult to delineate pulverization of their margins such as a rock-piece in the center of this photomicrograph.

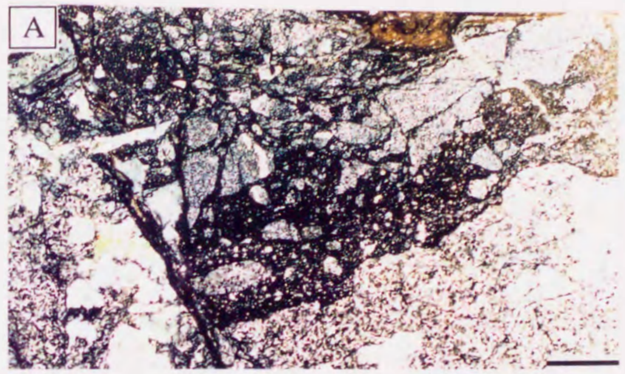

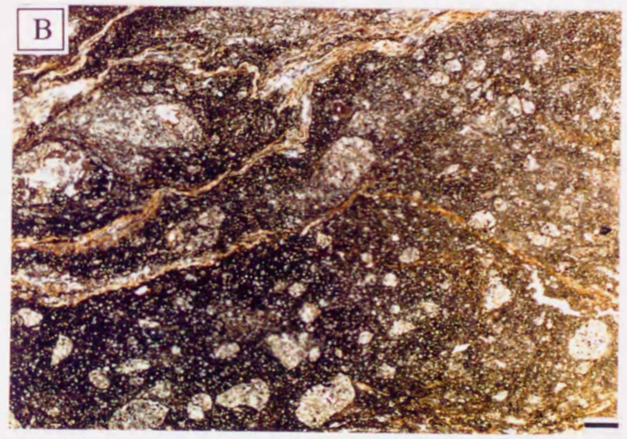

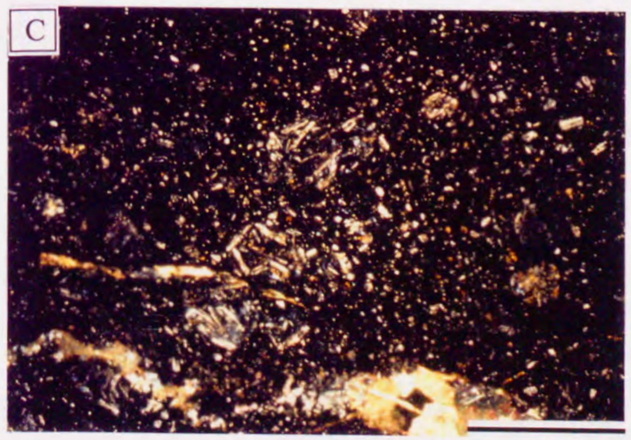

Plate 17

Plate 17 Photomicrographs of broken basalt-breccia. All scale bars: 1mm.
Localities are shown in Fig. 6.

A. Broken basalt breccia having two kinds of matrices of pulverization paste of different grain-sizes. Two kinds of pulverization paste: black part and dark brown part are complexly intermixed with each other and contain rock-pieces of basalt lava of several different destruction fabrics. Plane light.

B. Rock-piece of crushed basalt lava. Laths of plagioclase are completely pulverized into fine fragments. The boundary between the rock-piece and surrounding matrix of pulverization paste is distinct. Polars crossed.

C. Close-up view of rock-piece of brecciated basalt lava. Plane light.

D. Close-up view of the boundary between two kinds of pulverization paste. Light brown coarser pulverization paste of basaltic rocks in the center of the photograph is in distinct, unsheared, and irregularly-rugged contact with surrounding black finer pulverization paste. Varieties of pulverization paste form matrix of broken basalt-breccia. Polars crossed.

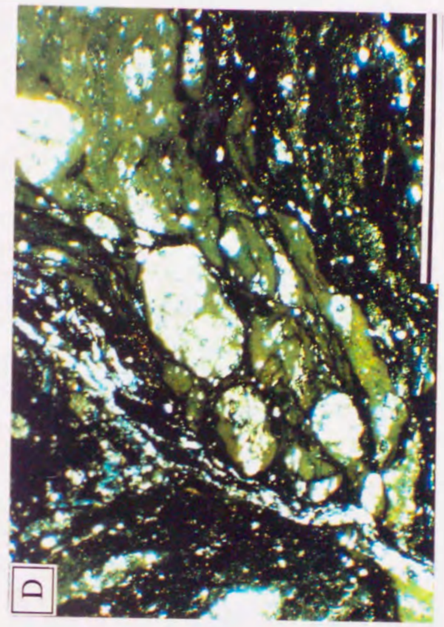

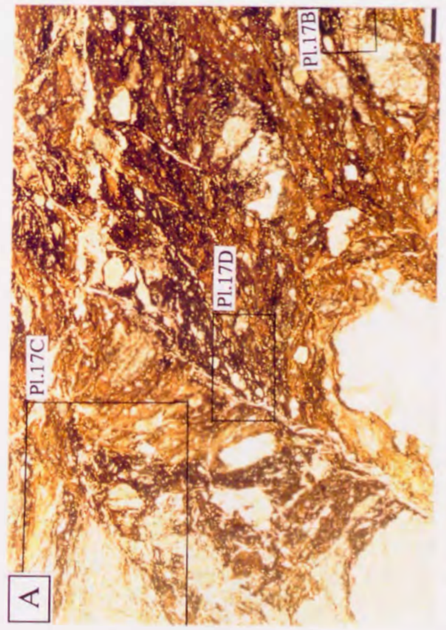

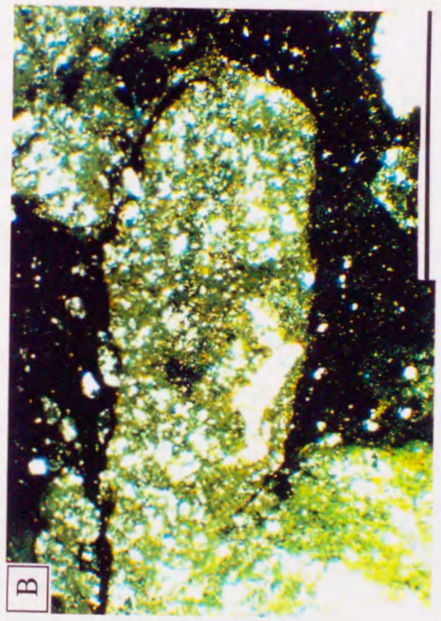

Plate 18

Plate 18 Photomicrographs of broken basalt-breccia containing limestone clasts. All scale bars: 1mm. Localities are shown in Fig. 6.

A. Broken basalt-breccia containing clasts of Permian shallow-marine limestone. Limestone clasts and rock-pieces of brecciated basalt lava are densely packed, disorganized and supported by each other. Black fine pulverization products of basaltic rocks are recognized. Plane light.

B. Limestone clasts injected by surrounding pulverization paste of basaltic rocks. Injection of pulverization products separates limestone clasts into two rock-pieces: a and b. Plane light.

C. Close-up view of injection of fine pulverization paste of basaltic rocks. Polars crossed.

D. Injection of pulverization products containing limestone rock-pieces separated from a larger clast (indicated by black arrows). Plane light.

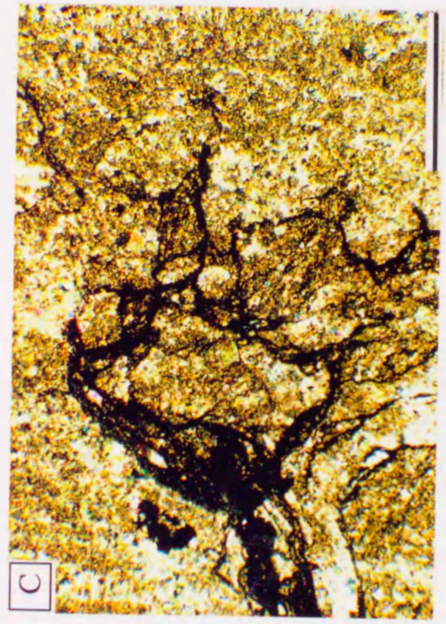

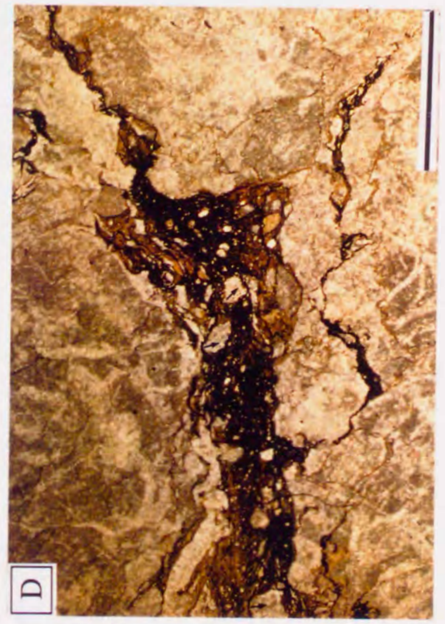

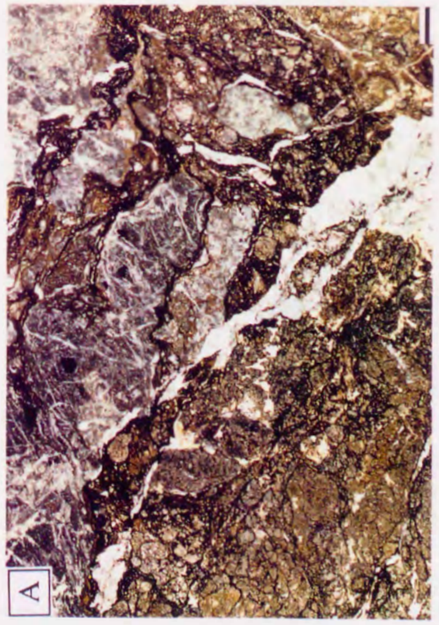

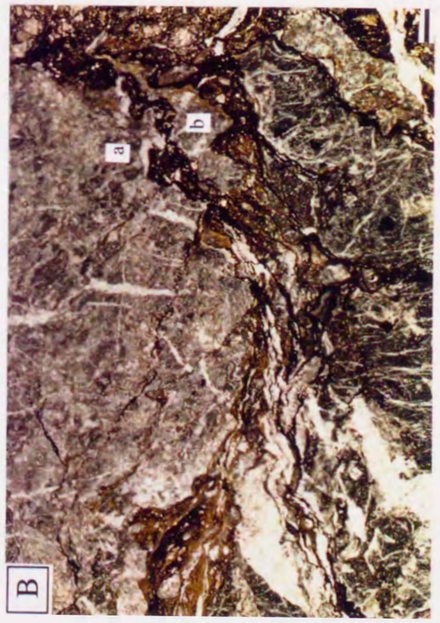

Plate 19

Plate 19 Broken basalt-breccia. Localities are shown in Fig. 6.

A. Outcrop view of the broken basalt-breccia (br.) containing blocks of basalt lava (b.).

B. Outcrop view of the broken basalt-breccia containing limestone blocks. Limestone blocks (gray) vary in size and shape, disorganized, and randomly embedded in broken basalt-breccia.

C. Polished slab of the broken basalt breccia. Destruction products of basaltic rocks show various fabrics of destruction resulting in their color-difference: a, b, and c. The finer pulverization products are much darker. Scale bar: 2 cm.

A

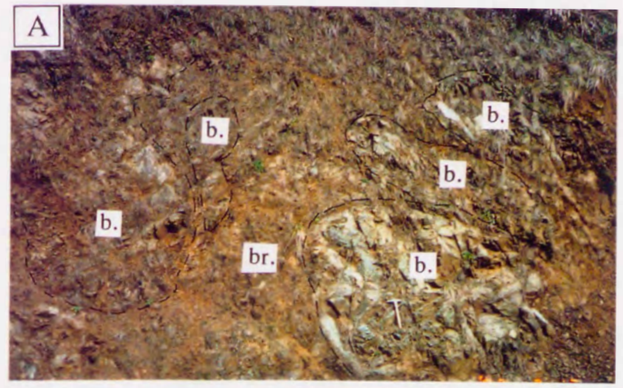

B

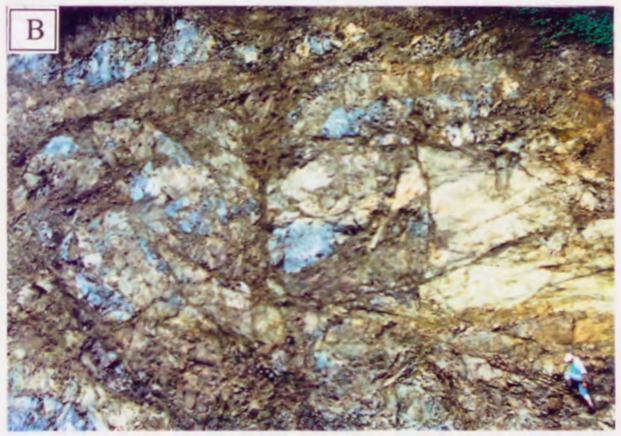

C

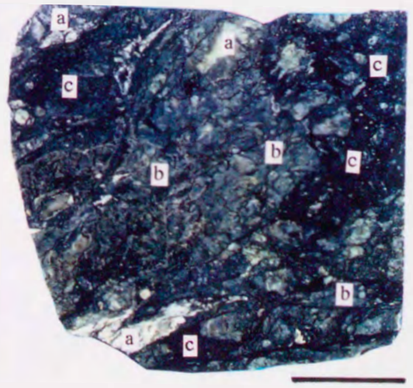

Plate 20

Plate 20 The boundary between Jurassic terrigenous sediments and broken basalt-breccia. Localities are shown in Fig. 6.

A. Outcrop view of the black mudstone (a) of the Hikone unit intercalated by broken basalt-breccia (b) of the Suzuka unit. Black mudstone yields radiolarian fossils of the *Tricolocapsa conexa* Zone indicative of early Late Jurassic.

B. Outcrop view of the boundary between the Hikone and Suzuka units. Black mudstone (a) of the Hikone unit and broken basalt-breccia (b) of the Suzuka unit are injected into each other along their boundary.

C. Photomicrograph of the boundary between the black mudstone and the broken basalt-breccia containing limestone clasts. Limestone clasts (c) enclosed by very fine pulverized basalt (b) containing plagioclase grains, which is in unsheared contact with black mudstone (a). Scale bars 1mm. Plane light.

D. Photomicrograph of a close-up view of the stylolitized, distinct boundary between the black mudstone (a) and the pulverization paste of basaltic rocks (b) with limestone clasts (c). Note that a small amount of detrital quartz (indicated by white arrows in Plate 20D) is scattered in fine pulverization paste of basaltic rocks. Scale bars: 1mm. Polars crossed.